A HOLLY-LEAF-SHAPED MONOPOLE ANTENNA WITH LOW RCS FOR UWB APPLICATION

H.-Y. Xu[*], H. Zhang, K. Lu, and X.-F. Zeng

Missile Institute of Airforce Engineering University, Sanyuan, Shaanxi 713800, China

Abstract—As to low observable platform, one of the major contributing sources of target RCS is the scattering due to onboard antennas. So the research on RCS reduction of the antenna is important. In this paper, a holly-leaf-shaped monopole antenna with low RCS is designed. A square notch is etched to improve impedance matching and expand the bandwidth in the ground. The measured $-10\,\text{dB}$ bandwidth is from 2.1 to 15.4 GHz (only a little higher than $-10\,\text{dB}$ around 7.5 GHz). The radiation patterns retain symmetry and are relatively stable at 2.5, 8 and 11 GHz. The monostatic RCS performance in four different incident cases is studied to obtain some helpful conclusions for the RCS reduction of the UWB antenna. The RCS achieves effective reduction in comparison with that of the reference antenna. The largest reduction is 4.1, 19.8, 3.9 dBsm in three different incident cases, respectively, while the largest loss of gain is only about $-1.3\,\text{dB}$. The antenna suits the occasion of desiring UWB antenna with low RCS.

1. INTRODUCTION

As a basic parameter that weighs up the exposure characteristic in the radar detection and stealth technology, radar cross section (RCS) [1–4] is a measure of power scattered by the target towards the illuminator. RCS reduction aims to control and reduce RCS of the military target to make it difficult to be discovered. Many military platforms are required to exhibit a low radar cross section in order to avoid detection by radar. The RCS of sensitive targets has been reduced considerably in recent years. As to low observable platform, one of the major contributing sources of target RCS is the scattering due to onboard

antennas. But conventional radar absorbing materials (RAM) coating techniques cannot be applied in this situation, as they will severely degrade the antenna performance. So RCS reduction of the antenna has become an important task to be solved. The related study is becoming a hot topic [5–9].

The ultra-wideband (UWB) radar and communication systems in the close quarters have the advantages of ultra-wideband spectrum and high resolving distance capability, which determine the ability of the accurate target identification and acquisition of fine characteristics of the complex objects. They have promising application values in the stealth and anti stealth domains. The ultra-wideband antenna [10–13] is a key component in developing the UWB technique. But it is very difficult to reduce the RCS of the UWB antenna due to the ultra-wide bandwidth. So the research on UWB antenna with low RCS is very valuable [14–17].

The printed monopole antennas have the merits of wide band, low cost, light weight, satisfactory radiation pattern and easy manufacturing. But its high RCS usually limits its application in stealth platforms [18–21]. In this paper, a novel monopole antenna with low RCS is designed. The antenna is composed of a holly-leaf-shaped radiating patch and a ground with a square notch which are located at the two sides of the substrate respectively. This paper analyzes both the radiating and scattering characteristics. The simulated and measured results show the antenna has obtained not only broad bandwidth but also low RCS almost in the whole operating band in comparison with the reference antenna.

2. THEORY ANALYSIS

The total scattering field $(\mathbf{E}^s(\vec{\mathbf{Z}}_l))$ can be divided into two categories: scattering of structural mode $(\mathbf{E}^s(\vec{\mathbf{Z}}_c))$ and antenna mode $(\vec{\mathbf{E}}^a(\mathbf{Z}_l))$. The scattering field of structural mode is determined by the structural characteristics such as antenna type, geometry, and material constitutions. That of antenna mode, which will change with different kinds of loads, lies on the reflection coefficient of the transmitter or receiver at the feed-in port. Their relationship is given by [22]

$$\mathbf{E}^s(\vec{\mathbf{Z}}_l) = \mathbf{E}^s(\vec{\mathbf{Z}}_c) + \vec{\mathbf{E}}^a(\mathbf{Z}_l) = \mathbf{E}^s(\vec{\mathbf{Z}}_c) + \frac{\Gamma_l}{1 - \Gamma_l\Gamma_a}\mathbf{b}_0^m\mathbf{E}_1^t \qquad (1)$$

where $\mathbf{Z}_l$ is the port load, $\mathbf{Z}_c$ is the antenna intrinsic impedance, Γ_l is the antenna reflection coefficient, Γ_a is the load reflection coefficient of the receiver, $\mathbf{b}_o^m$ is the scattering incepting matching amplitude when

the antenna port is with matched load, $\vec{\mathbf{E}}_1^t$ is the radiating electric field with the unit excitation.

For $\mathbf{Z}_l = 0$

$$\Gamma_l = \frac{\mathbf{Z}_l - \mathbf{Z}_c}{\mathbf{Z}_l + \mathbf{Z}_c} = \frac{0 - \mathbf{Z}_c}{0 + \mathbf{Z}_c} = -1 \tag{2}$$

Substituting $\mathbf{Z}_l = 0$ and $\Gamma_l = -1$ into formula (1) yields

$$\mathbf{E}^s\vec{\,}(0) = \mathbf{E}^s\,(\vec{\mathbf{Z}}_c) - \frac{1}{1+\Gamma_a}\mathbf{b}_0^m\mathbf{E}_1^t \tag{3}$$

For $\mathbf{Z}_l = \infty$

$$\Gamma_l = \frac{\mathbf{Z}_l - \mathbf{Z}_c}{\mathbf{Z}_l + \mathbf{Z}_c} = \frac{\infty - \mathbf{Z}_c}{\infty + \mathbf{Z}_c} = 1 \tag{4}$$

Substituting $\mathbf{Z}_l = \infty$ and $\Gamma_l = 1$ into formula (1) yields

$$\mathbf{E}^s\vec{\,}(\infty) = \mathbf{E}^s\,(\vec{\mathbf{Z}}_c) + \frac{1}{1-\Gamma_a}\mathbf{b}_0^m\mathbf{E}_1^t \tag{5}$$

Solve Eqs. (3) and (5), scattering field $\mathbf{E}^s(\mathbf{Z}_c)$ and $\mathbf{b}_0^m\mathbf{E}_1^t$ can be obtained as:

$$\mathbf{E}^s\,(\mathbf{Z}_c) = \frac{(1-\Gamma_a)\,\mathbf{E}^s\,(\infty) + (1+\Gamma_a)\,\mathbf{E}^s\,(0)}{2} \tag{6a}$$

$$\mathbf{b}_0^m\mathbf{E}_1^t = \frac{1-\Gamma_a^2}{2}\,[\mathbf{E}^s\,(\infty) - \mathbf{E}^s\,(0)] \tag{6b}$$

Substituting (6a) and (6b) into Eq. (1) yields

$$\mathbf{E}^s(\mathbf{Z}_l)$$
$$= \frac{(1-\Gamma_a)\mathbf{E}^s(\infty)+(1+\Gamma_a)\mathbf{E}^s(0)}{2} + \frac{\Gamma_l}{1-\Gamma_a\Gamma_l}\frac{1-\Gamma_a^2}{2}\,[\mathbf{E}^s(\infty)-\mathbf{E}^s(0)] \tag{7}$$

where $\mathbf{E}^s(\infty)$ and $\mathbf{E}^s(0)$ are the scattering field with open and short load at the feed-in port respectively. As can be seen from formula (7), the antenna scattering field with arbitrary load can be obtained by that of open and short circuits. What's more, the phase difference between the RCS of structural mode and that of the antenna mode can be easily deduced from (1), (6a) and (6b).

3. ANTENNA GEOMETRY

The geometries of the holly-leaf-shaped and reference antennas are shown in Figs. 1(a) and (b), respectively. As shown in Fig. 1(a), the holly-leaf-shaped antenna is printed on the FR-4 substrate with the thickness of 0.8 mm and relative dielectric constant of 4.6. The radiating patch and ground plane are printed on the two sides of
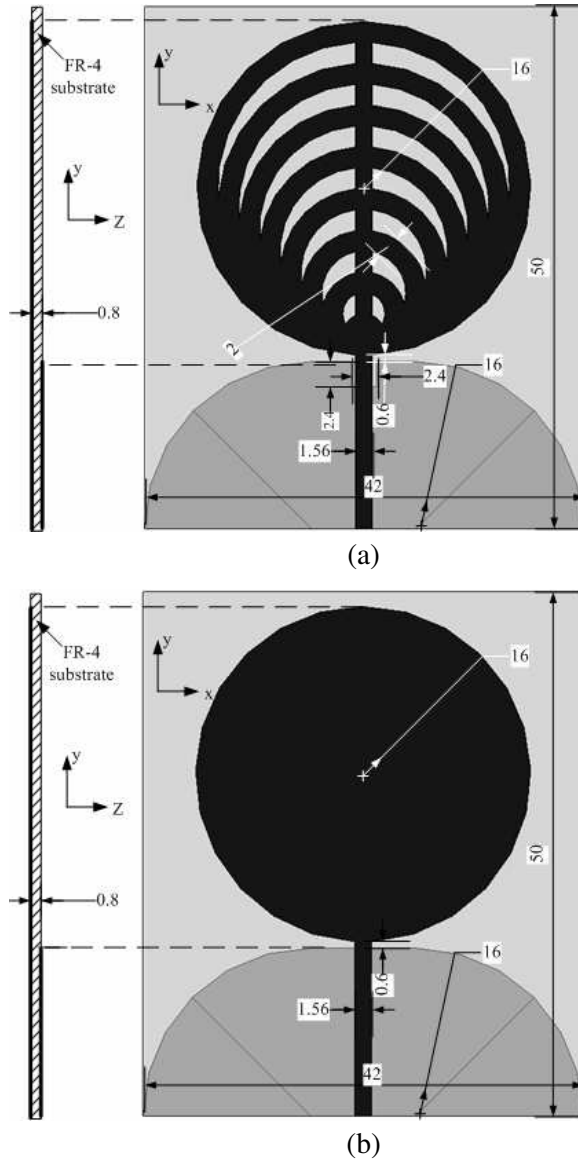
(a)

(b)

Figure 1. Geometries of the antennas: (a) holly-leaf-shaped antenna, (b) reference antenna.

the substrate, respectively. Based on the bionics principle and the model of holly leaf, the radiating patch is composed of a rectangle and several tangential circle loops with the equal width to look something

like the holly leaf. The ground plane is smoothed at the left and right edges to prevent the radiation beam to be gradient. There is a square notch in the ground for adjusting the gap between the radiating element and ground to improve the matching and bandwidth. Fig. 1(b) is the geometry of the reference antenna, which is a slightly modified geometry of the antenna in [17]. Its substrate is the same as that of the novel antenna. The sizes of the two antennas are both $50 \, \text{mm} \times 42 \, \text{mm} \times 0.8 \, \text{mm}$.

4. PERFORMANCE AND ANALYSIS

Because the radiation and scattering performance of antennas nearly can't enhance at the same time, the principle of designing this antenna is to find ways to reduce the RCS at the premise of basically maintaining the bandwidth and radiation characteristic. It is well known that two different biologic objects with similar sizes usually have completely different RCS. Based on bionics principle, the geometry of the proposed antenna in Fig. 1(a) is designed to look something like the holly leaf to have less metal area than the reference antenna in Fig. 1(b), as a result of which, the RCS of the antenna can be reduced effectively. On the other hand, a square notch is etched to improve the impedance bandwidth in the ground.

4.1. Impedance Bandwidth

As shown in Fig. 2, the $-10 \, \text{dB}$ simulated impedance bandwidth of the holly-leaf-shaped antenna is from $2 \, \text{GHz}$ to more than $11 \, \text{GHz}$ which is wider than that of the reference antenna. What's more, the return loss of the reference antenna is a little more than $-10 \, \text{dB}$ around $3 \, \text{GHz}$ and $8.2 \, \text{GHz}$. All simulations in this paper are performed by HFSS software.

The holly-leaf-shaped monopole antenna is fabricated and measured. As shown in Fig. 3, two curves have similar shape. The measured result shows that the return loss is below $-10 \, \text{dB}$ from 2.1 to $15.4 \, \text{GHz}$ (only a little higher than $-10 \, \text{dB}$ around $7.5 \, \text{GHz}$). The measured bandwidth is wider than the simulated result, which may be due to a larger $\tan \delta$ of the substrate and the fabrication error.

4.2. Radiating Performance

The radiation patterns of the holly-leaf-shaped antenna are given in Fig. 4, which shows that the measured and simulated results are basically consistent. And the radiation patterns retain very
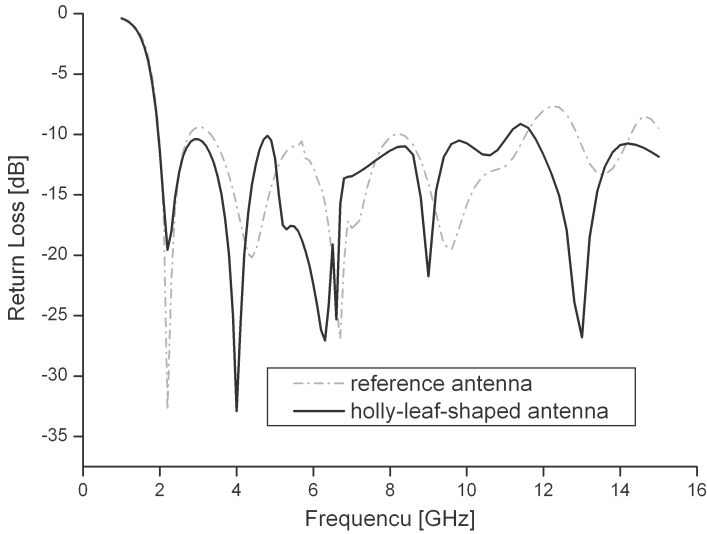
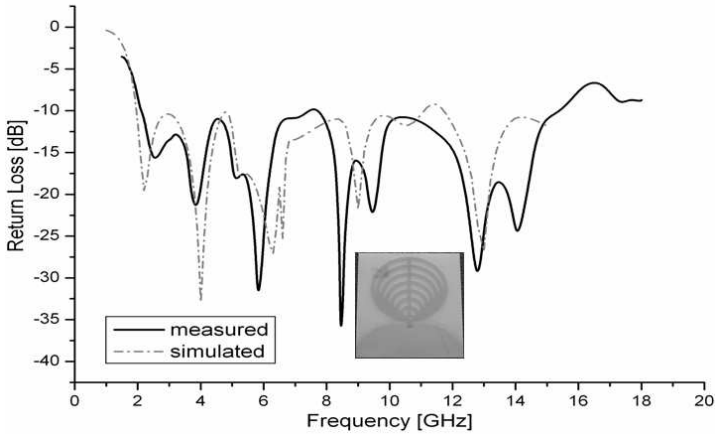**Figure 2.** Simulated return loss of the two antennas.

Figure 3. Measured and simulated results of the holly-leaf-shaped antenna.

symmetrical and are relatively stable. Figs. 4(a), (b), (c) and (d) show that the measured and simulated results are basically consistent at 2.5 GHz and 8 GHz. Figs. 4(e), (f) are the simulated radiation patterns of the E-plane and H-plane at 11 GHz, respectively, which show that the radiation patterns still retain symmetrical very well at
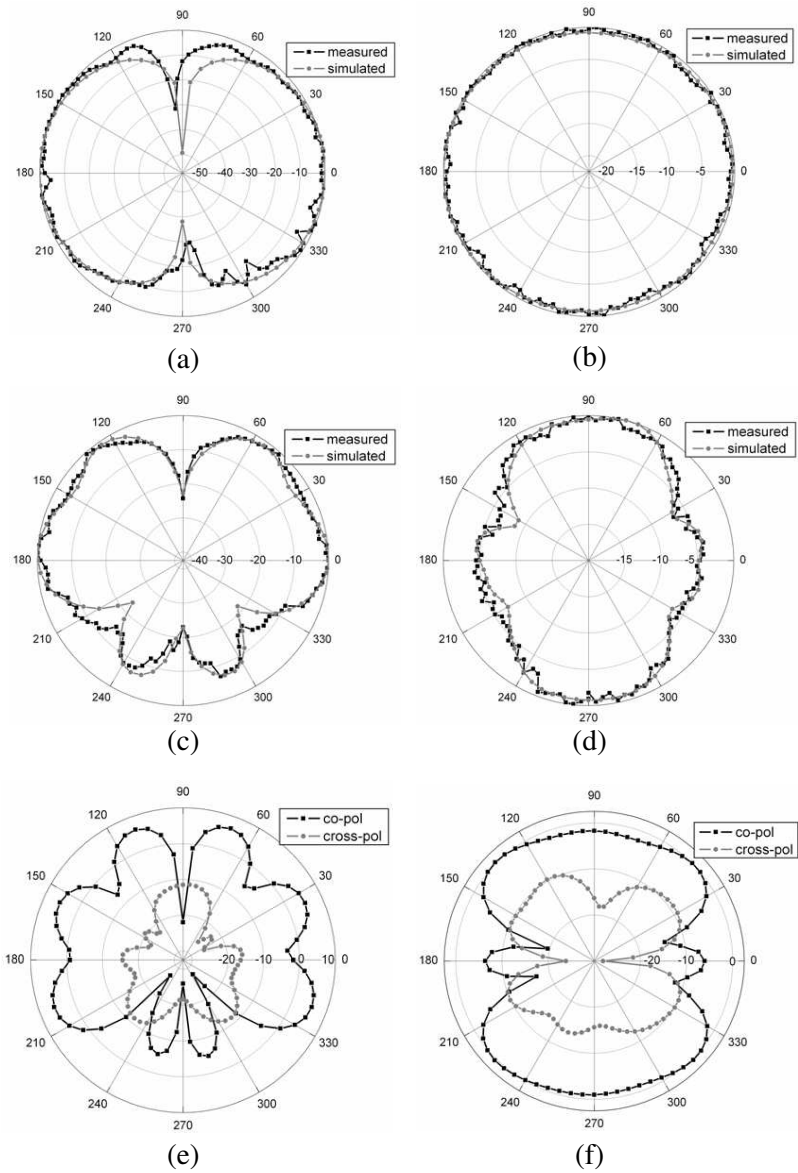
Figure 4. Radiation patterns at (a) 3 GHz E-plane, (b) 3 GHz H-plane, (c) 8 GHz E-plane, (d) 8 GHz H-plane, (e) 11 GHz E-plane and (f) 11 GHz H-plane.
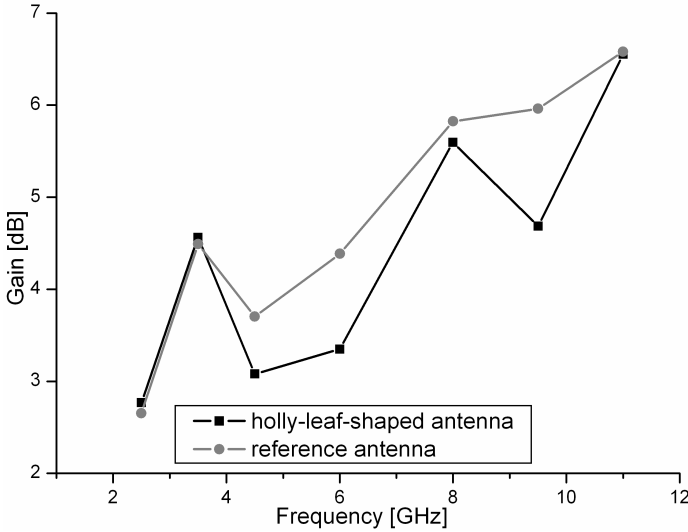
Figure 5. Gain comparison.

high frequency.

The gain comparison of the two antennas is shown in Fig. 5. It can be shown that the gain of the holly-leaf-shaped antenna is lower than that of the reference antenna almost in the whole operating band. The largest gain loss is about -1.3 dB at 9.5 GHz. This loss should be caused by the area reduction of the radiating patch.

4.3. Scattering Performance for the Case of k Vector (0, 0, -1) and E Vector (0, 1, 0)

Figure 6 gives the monostatic RCS curves of the holly-leaf-shaped and reference antenna, which are both with matched load ($50\,\Omega$) at the feed-in port. So it can be deduced from formula (1) that the values of the RCS are mainly given by that of the structural mode in this situation. As shown in Fig. 6, the holly-leaf-shaped antenna has lower RCS in the frequency band of 1.5–3.3 GHz and 5–13.4 GHz while the reference antenna only has lower RCS in the range of 3.3–5 GHz. It is apparent of the RCS reduction in the range of 5–13.4 GHz. The largest reduction is about 4.1 dBsm at 5.1 GHz. E vector of both the incident and received electric fields in Figs. 6 and 7 is $(0, 1, 0)$. K vector of the incident waves is $(0, 0, -1)$.

Figure 7 is the monostatic RCS of the holly-leaf-shaped antenna with different kinds of loads. As shown in Fig. 7, there is no kind
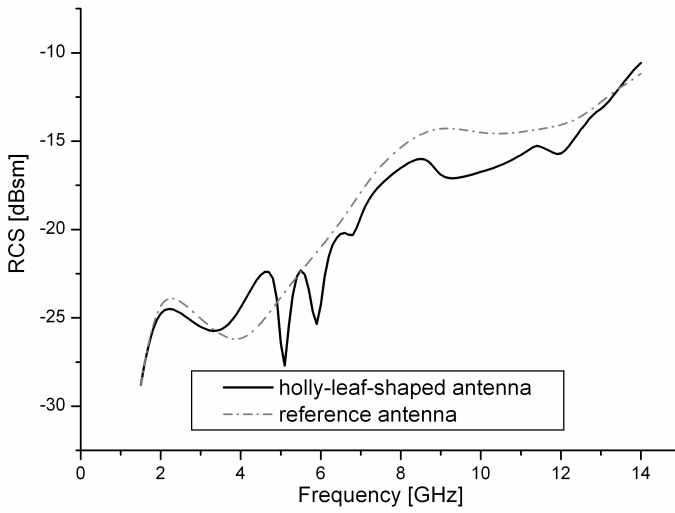
Figure 6. Comparison of the RCS with k vector $(0, 0, -1)$ and E vector $(0, 1, 0)$.
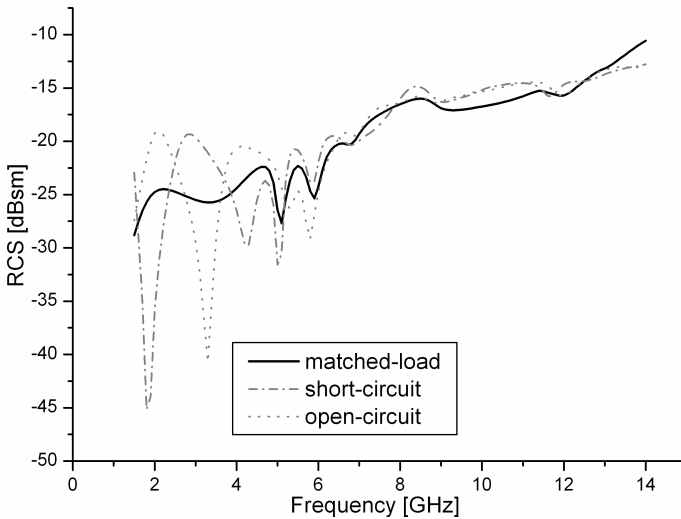

Figure 7. RCS of the holly-leaf-shaped antenna with different loads with k vector $(0, 0, -1)$ and E vector $(0, 1, 0)$.
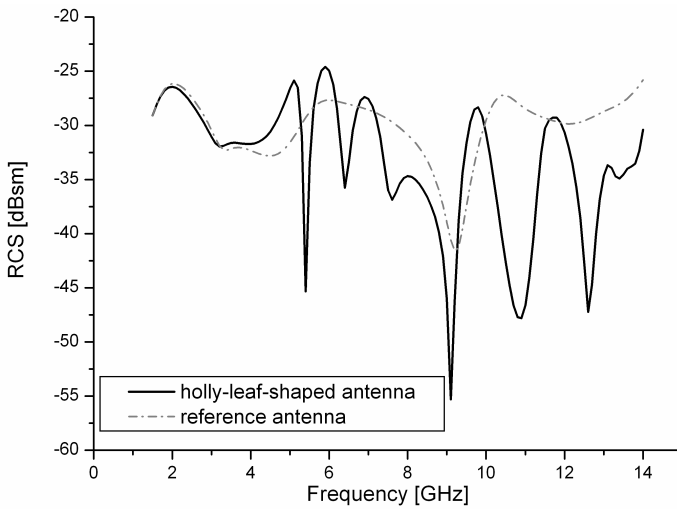
Figure 8. Comparison of the RCS with k vector $(-1, 0, 0)$ and E vector $(0, 1, 0)$.

of load can always keep the RCS the largest or lowest in the whole UWB operating frequency band, which greatly increases the difficulty of reducing the RCS of the UWB antenna. This is because the UWB antenna has much wider bandwidth than the narrow band antenna to make the shift of phase difference between the antenna mode and the structural mode scattering field much lager.

4.4. Scattering Performance for the Case of k Vector $(-1, 0, 0)$ and E Vector $(0, 1, 0)$

Figure 8 shows the RCS comparison of the two antennas with matched load $(50\,\Omega)$ at the feed-in port with the incident waves k vector $(-1, 0, 0)$ and the incident and received electric fields E vector $(0, 1, 0)$. It is seen that the RCS of the holly-leaf-shaped antenna has obtained some reduction in most of the frequency band. The reduction around 5.4 GHz, 9.1 GHz, 11 GHz, 12.6 GHz is obvious. The largest reduction is about 19.8 dBsm at 12.6 GHz.

Figure 9 is the monostatic RCS of the holly-leaf-shaped antenna with different kinds of loads for the case of k vector $(-1, 0, 0)$ and E vector $(0, 1, 0)$, which also reveals that no kind of load can assure the RCS highest or lowest in the whole operating band.
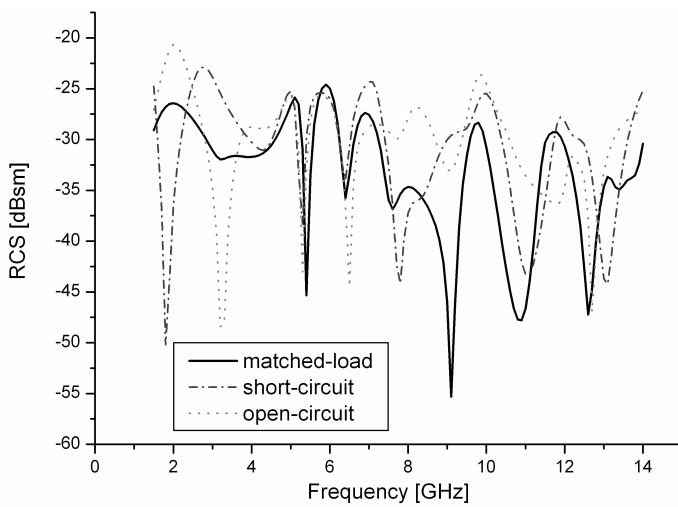
Figure 9. RCS of the holly-leaf-shaped antenna with different loads with k vector $(-1, 0, 0)$ and E vector $(0, 1, 0)$.
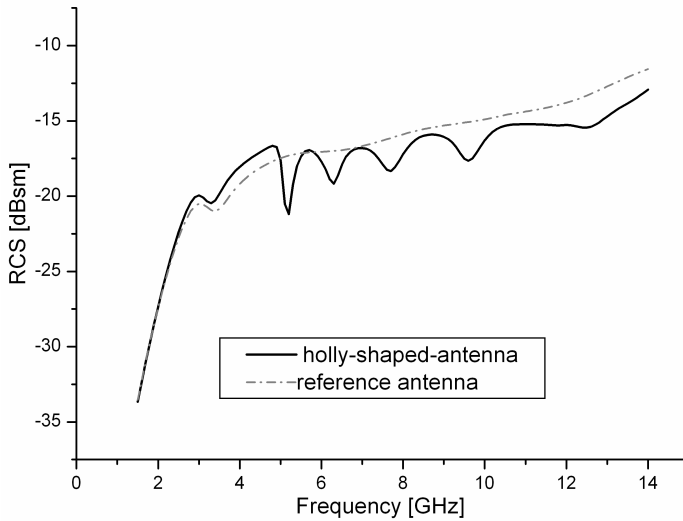

Figure 10. Comparison of the RCS with k vector $(0, 0, -1)$ and E vector $(1, 0, 0)$.

4.5. Scattering Performance for the Case of k Vector $(0, 0, -1)$ and E Vector $(1, 0, 0)$

Figure 10 gives the RCS comparison of the two antennas with matched load $(50\,\Omega)$ at the feed-in port with k vector $(-1, 0, 0)$ and and E vector

$(1, 0, 0)$. It can be seen that the RCS of the holly-leaf-shaped antenna has obtained effective reduction in most of the frequency band. The largest reduction is about 3.9 dBsm. Because the incident electric field is perpendicular to the co-polarization of the antenna, the induced current can't arrive at the feed-in port to induce the scattering field of antenna mode. In this case, the scattering field of structural mode should be the main contribution to the total scattering field.

As can be seen from Fig. 11, the RCS of the holly-leaf-shaped antenna with different loads are almost the same in the whole frequency band, which has proved that the RCS with k vector $(0, 0, -1)$ and E vector $(1, 0, 0)$ is mainly composed of that of the structural mode.

4.6. Scattering Performance for the Case of k Vector $(-1, 0, 0)$ and E Vector $(0, 0, 1)$

Fig. 12 shows that the RCS values of two antennas are both below -45 dB in the frequency band. It is because there is no induced current on the metal with the incident normal E vector $(0, 0, 1)$, and as a result, the RCS of the substrate is the main contribution to the total.

Figure 13 shows the RCS curves with different loads which are all very low. It can be concluded from formula (7) that the RCS values of the antenna with arbitrary load are mainly the contribution of the
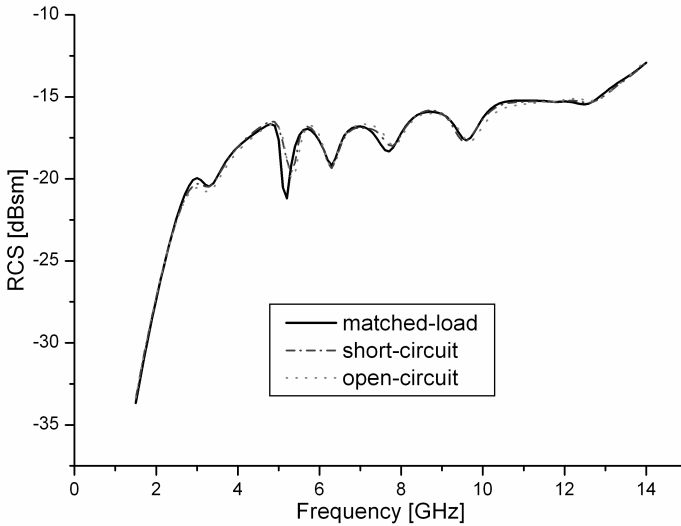

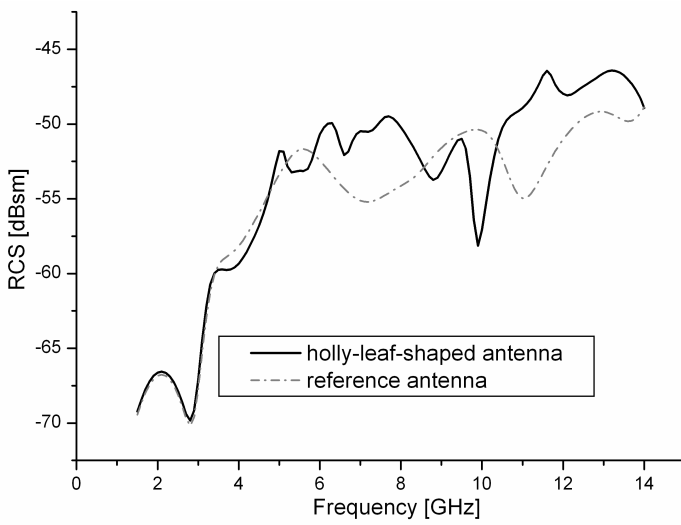**Figure 11.** RCS of the holly-leaf-shaped antenna with different loads with k vector $(0, 0, -1)$ and E vector $(1, 0, 0)$.

Figure 12. Comparison of the RCS with k vector $(-1, 0, 0)$ and E vector $(0, 0, 1)$.
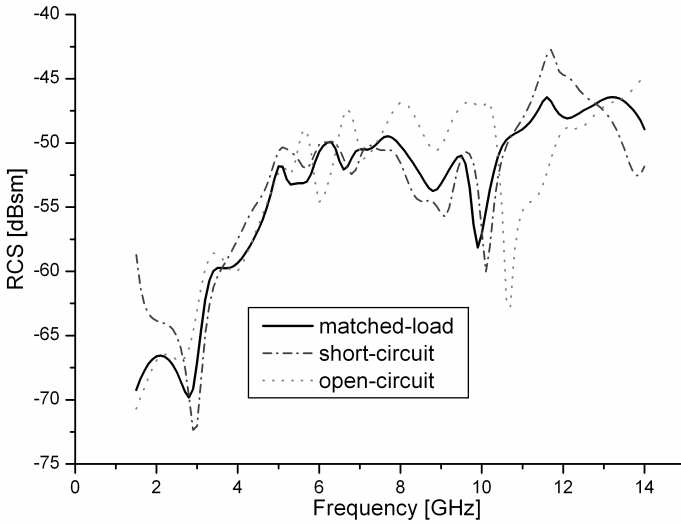

Figure 13. RCS of the holly-leaf-shaped antenna with different load with k vector $(0, 0, -1)$ and E vector $(1, 0, 0)$.
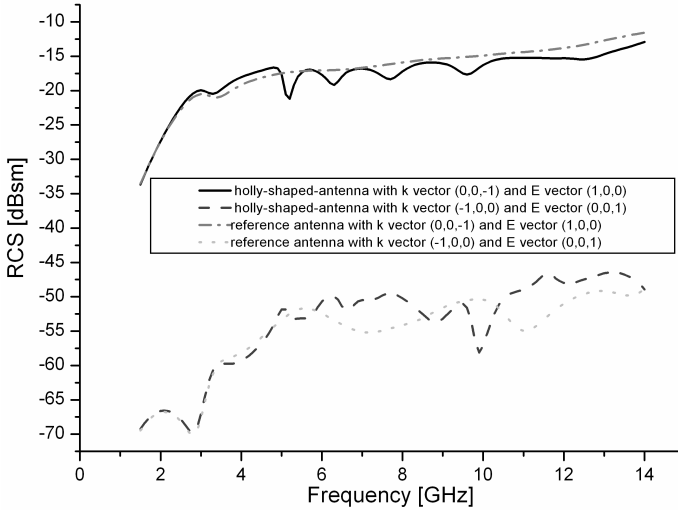
Figure 14. Comparison of the four RCS curves.

substrate for the case of k vector $(-1, 0, 0)$ and E vector $(0, 0, 1)$.

Figure 14 shows the comparison of four RCS curves. It can be concluded that the RCS values of any printed antennas should also be very low if the E vector is normal field.

5. CONCLUSION

Based on the bionics principle, a holly-leaf-shaped monopole antenna is proposed. The radiating patch is designed something like the holly leaf to balance the radiating and scattering performance. A square notch is etched in the ground to improve the matching and bandwidth. The simulated and measured results show that the holly-leaf-shaped antenna has wider impedance bandwidth than the reference antenna. The radiation patterns retain very symmetrical and are relatively stable.

The scattering performance is analyzed in four different incident cases. It can be concluded that the holly-leaf-shaped antenna has obtained lower RCS in most of the frequency band with the E vector parallel to the metal patch, the RCS with arbitrary load is mainly contributed by that of the structural mode for the case of the E vector perpendicular to the co-polarization of the antenna, and the RCS is very low with the incident normal electric field. The largest RCS reduction in three different incident cases has achieved 4.1, 19.8,

3.9 dBsm, respectively, while the largest gain loss is only about 1.3 dB.

The work in this paper may be helpful for the RCS reduction of the UWB antenna. This new design basically balances the radiating and scattering performance. So it is expected to be used in the occasion of desiring UWB antenna with low RCS.

REFERENCES

1. Wang, W.-T., S.-X. Gong, Y.-J. Zhang, F.-T. Zha, J. Ling, and T. Wan, "Low RCS dipole array synthesis based on MOM-PSO hybrid algorithm," *Progress In Electromagnetics Research*, Vol. 94, 119–132, 2009.

2. Cao, P. C., Y.-B. Tao, and H. Lin, "Fast RCS prediction using multiresolution shooting and bouncing ray method on the GPU," *Progress In Electromagnetics Research*, Vol. 107, 187–202, 2010.

3. De Cos, M. E., Y. Alvarez Lopez, and F. Las-Heras Andrés, "A novel approach for reduction using a combination of artificial magnetic conductors," *Progress In Electromagnetics Research*, Vol. 107, 147–159, 2010.

4. Sun, X. M., H. H. Wang, and H. Y. Zhang, "Scattering by an infinite cylinder arbitrarily illuminated with a couple of gaussian beams," *Journal of Electromagnetic Waves and Applications*, Vol. 24, No. 10, 1329–1339, 2010.

5. Li, H., B.-Z. Wang, G. Zheng, W. Shao, and L. Guo, "A reflectarray antenna backed on FSS for low RCS and high radiation performances," *Progress In Electromagnetics Research C*, Vol. 15, 145–155, 2010.

6. Hong, T., L.-T. Jiang, Y.-X. Xu, S.-X. Gong, and W. Jiang, "Radiation and scattering analysis of a novel circularly polarized slot antenna," *Journal of Electromagnetic Waves and Applications*, Vol. 24, No. 13, 1709–1720, 2010.

7. Liu, Y., S.-X. Gong, D.-M. Fu, "A novel model for analyzing the RCS of microstrip antenna," *IEEE Antennas and Propagation Society International Symposium*, Vol. 4, 835–838, 2003.

8. Heidrich. E. and W. Wiesbeck, "Reduction and minimization of antenna scattering," *IEEE Antennas and Propagation Society International Symposium*, Vol. 2, 904–907, 1992.

9. Zhao, S.-C. and B.-Z. Wang, "Advances on radar cross reduction of microstrip antenna array," *Systems Engineering and Eletronics*, Vol. 31, No. 4, 812–815, 2009.

10. Zhong, S.-S. and X.-L. Liang, "Progress in ultra-wideband planar

antennas," *Journal of Shanghai University (English Edition)*, Vol. 11, No. 2, 95–101, 2007.

11. Lv, W.-J. and H.-B. Zhu, "On the frequency notched planar ultra-wideband antennas," *Chinese Journal of Radio Science*, Vol. 24, No. 4, 780–785, 2009 (in Chinese).

12. Sze, J.-Y., K.-L. Wong, and C.-C. Huang, "Coplanar waveguide-fed square slor antenna for broadband circularly polarized radiation," *IEEE Transactions on Antennas and Propagation*, Vol. 51, No. 8, 2003.

13. Xia, Y.-Q., J. Luo, and D.-J. Edwards, "Novel miniature printed monopole antenna with dual tunable band-notched characteristics for UWB applications," *Journal of Electromagnetic Waves and Applications*, Vol. 24, No. 13, 1783–1793, 2010.

14. Xu, H.-Y., H. Zhang, X. Yin, and K. Lu, "Ultra-wideband Koch fractal antenna with low backscattering cross section," *Journal of Electromagnetic Waves and Applications*, Vol. 24, Nos. 17–18, 2615–2623, 2010

15. Jiang, W., S.-X. Gong, T. Hong, and X. Wang, "Fan-shaped antenna with low RCS for ultra-wideband application," *Acta Electronica Sinica*, Vol. 38, No. 9, 2162–2165, 2010 (in Chinese).

16. Liu, Y. and S. X. Gong, "A novel UWB clover-disc monopole antenna with RCS reduction," *Journal of Electromagnetic Waves and Applications*, Vol. 22, Nos. 8–9, 1115–1121, 2008.

17. Hu, S., H. Chen, and C. L. Law, "Backscattering cross section of ultra-wideband antennas," *IEEE Antennas and Wireless Propagation Letter*, Vol. 6, 70–73, 2007.

18. Huang, C.-Y. and W.-C. Hsia, "Planar elliptical antenna for ultra-wideband communications," *Electronic Letters*, Vol. 41, No. 6, 2005.

19. Yang, Z., L. Li, and H. Wang, "Investigation on ultra-wideband printed circular monopole antenna with frequency-notched," *IEEE ICMMT2008 Proceedings*, 2008.

20. Liang, J., C. C. Chiau, X. Chen, et al., "Study of a printed circular disc monopole antenna for UWB systems," *IEEE Transaction on Antennas Propagation*, Vol. 53, No. 11, 3500–3504, 2005.

21. Zhong, L.-L., J.-H. Qiu, and B. Sun, "Analysis and design of ultrawide-band circular antenna," Vol. 29, No. 4, 1387–1413, 2008 (in Chinese).

22. Gong, S.-X. and Y. Liu, *Prediction and Reduction of Antenna Radar Cross Section*, Publishing House of Xidian University, Xi'an, 2010.